Magnetic linear dichroism in x-ray emission spectroscopy: Yb in $Yb_3Fe_5O_{12}$

F. M. F. de Groot

Department of Inorganic Chemistry and Catalysis, Utrecht University, Sorbonnelaan 16, 3584 CA Utrecht, the Netherlands

M. H. Krisch and F. Sette

ESRF, BP 220, 38043 Grenoble, France

J. Vogel

Laboratoire Louis Néel (CNRS), 25, Avenue des Martyrs, BP 166, 38042 Grenoble, France

(Received 3 January 2000)

A magnetic linear dichroism MLD effect of up to 5% has been observed in the $2p_{1/2}4d$ x-ray emission spectrum of Yb in $Yb_3Fe_5O_{12}$. The spectral shape is well reproduced with an atomic multiplet calculation of the $4d$ to $2p$ decay. It is shown that the details of the spectral shapes are determined by the $4d4f$ exchange interaction. While the integrated intensity of the MLD effect is zero, the magnitude of the effect is a direct measure of the $4f$ magnetic moment of Yb. The technique is applicable to all rare-earth and transition-metal systems (probing the $3d$ magnetic moment). With respect to x-ray-absorption magnetic circular dichroism it possesses the advantage that (i) hard x rays are involved and (ii) no circular polarization is needed. Therefore all complications related to electron detection, soft x-ray experiments, and circular polarization disappear. Potential applications include the study of (buried) magnetic systems *in situ*, at high pressures, varying (high) magnetic fields, and varying temperatures.

I. INTRODUCTION

The quantitative analysis of magnetic dichroic effects in x-ray absorption, photoemission, and x-ray emission spectra aims at the determination of element- and shell selective magnetic ground-state properties such as the orbital and spin magnetic moment or higher multipole moments. In particular absorption x-ray magnetic circular dichroism (X-MCD),[1] observed in 1987, is now a standard tool in the study of magnetism. Magnetic linear dichroism (MLD) effects were evidenced in x-ray-absorption spectroscopy (XAS),[2,3] and a few years later in angle integrated[4,5] and angular dependent photoemission spectroscopy.[6] For these spectroscopies the MLD effect identifies with the spectral dependence on the relative orientation of the magnetization vector with respect to the electric-field vector. In analogy with absorption and photoemission MLD, the x-ray emission MLD effect is the angular dependence of the x-ray emission cross section with respect to the magnetization vector. Moreover, there is, as for the other MLD phenomena, the possibility that the emission MLD effects are due to an anisotropic crystal field.[7,8] In contrast to X-MCD in x-ray emission that has been dealt with in theory and experiment,[9–11] there exists to our knowledge no work concerning linear dichroism effects.

In this paper, we report the detection of a magnetic linear dichroism effect in the Yb $2p_{1/2}4d$ x-ray emission spectrum of $Yb_3Fe_5O_{12}$. In Sec. II we describe the experimental setup and present the results. Section III deals with the theoretical simulation of the spectral shape within the framework of an atomic multiplet model and the comparison with the experimental spectrum. Section IV contains the discussion, where specific emphasis is put on the similarities and complementarities between linear and circular magnetic dichroism in x-ray emission. The paper concludes with Sec. V where we

outline some potential applications of this interesting technique.

II. EXPERIMENT

The experiment was performed on the inelastic x-ray scattering beamline ID16 at the European Synchrotron Radiation Facility (ESRF). The incident linearly polarized x rays produced by a linear 42-mm undulator were monochromatized by a cryogenically cooled silicon (111) double crystal monochromator, providing an energy bandwidth of approximately 1.5 eV. The beam impinging on the sample was sized down to 0.6 mm horizontally by 2 mm vertically. These settings resulted in an incident photon flux of 3×10^{12} photons/sec. The scattered radiation was analyzed in the horizontal plane by a 1-m Rowland circle spectrometer, utilizing the (660) reflection order from a spherically bent silicon crystal. The solid angle spanned by the analyzer crystal was 3.6 mrad^2. The overall experimental resolution was 2.3 eV. The $Yb_3Fe_5O_{12}$ sample was mounted inside a closed-cycle helium cryostat and kept at 90 K. A magnetic field of 0.3 T was applied perpendicular to the sample surface and parallel to the incident photon beam direction. X-ray emission spectra were recorded at 110° and 150° scattering angle, corresponding to an angle between the magnetic field direction and the emitted x rays of 70° and 30°, respectively.

The top panel of Fig. 1 shows the $2p_{1/2}4d$ x-ray emission spectral shape measured at angles of $\theta = 30°$ (dashed) and $\theta = 70°$ (solid). The excitation energy was 10 070 eV, some 100 eV above the YbL_2 edge. The emission line is composed of three features: a main line, centered around 9775.5 eV, a shoulder at 9770 eV, and a well resolved satellite at 9785 eV. The difference of the two spectra manifests itself in the intensity ratio between the main line and the shoulder, while
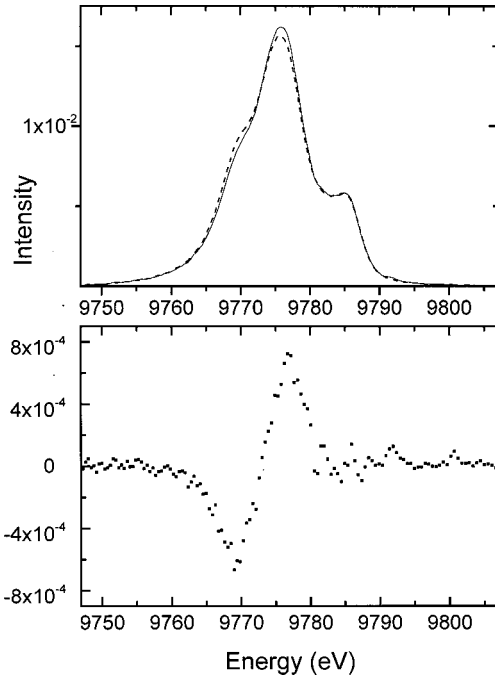
FIG. 1. Top: the $2p_{1/2}4d$ x-ray emission spectral shape as a function of x-ray emission energy at detection angles of $\theta=30°$ (dotted line) and $\theta=70°$ (solid line). Bottom: difference spectrum ($\theta=70° - \theta=30°$).

there is no detectable difference at the satellite position. This is illustrated in the difference spectrum that is displayed in the bottom panel of Fig. 1. The maximum of the linear magnetic dichroism effect amounts to about 5%. We note that the integrated intensity of the spectra is equal for the two detection angles, which offers an additional normalization check. Spectra recorded with an unmagnetized sample at the two selected scattering angles did not display any detectable dichroic effect. The $2p_{1/2}4d$ x-ray emission spectral shape is determined by the strong $4d4f$ interactions in the $4d^9 4f^{13}$ final state. These interactions, in particular the $4d4f$ exchange interaction, spread out the spectrum over some 20 eV. Before analyzing the MLD effects, in the next section we will describe the procedure to simulate the spectral shapes.

III. THEORY

The Yb $2p_{1/2}4d$ x-ray emission spectral shape is calculated using an atomic multiplet model.[3,11] Yb is described only including the $4f$ electrons in their $^2F_{7/2}$ Hund's rule ground state. The intensity of the x-ray emission process is given by the Kramers-Heisenberg formula,[12] describing the resonant inelastic scattering process, characterized by the transition from the initial to the final state via a resonant intermediate state:

$$I_{(\hbar\omega, \hbar\omega')} = \sum_{q'} \sum_{q} F_{q'q} \cdot \delta_{E_f + \hbar\omega' - E_0 - \hbar\omega}. \qquad (1)$$

The sum extends over the incoming (q) and emitted (q') photon polarization states. The δ function assures energy conservation by stating that the difference between the final-state energy E_f and the ground-state energy E_0 equals the

difference of incident to scattered photon energy. If the intermediate states can be approximated as independent states, the Kramers-Heisenberg formula can be simplified into a two-step formula removing the complications of interference:[11]

$$F_{q'q} = \sum_{4d^9 4f^{13}} |\langle 4d^9 4f^{13} | C_{q'} | 2p^5 4f^{13} \rangle|^2$$

$$\times \sum_{\varepsilon} |\langle 2p^5 4f^{13} + \varepsilon | C_q | 4f^{13} \rangle|^2. \qquad (2)$$

The second matrix element denotes the excitation step, involving the promotion of a $2p$ electron into a continuum state (ε). The continuum electron is omitted in the calculation of the decay step. C_q and $C_{q'}$ are the dipole transition operators of the excitation and the emission process, respectively, expressed as normalized spherical harmonics. In off-resonance excitation, the $2p4d$ x-ray emission spectral shape can be approximated as the product of x-ray-absorption and x-ray emission intensities, in which the matrix element of the excitation step enters only as a constant. The angle between the magnetic field direction and the emitted x rays is defined as θ, with the angular dependence of the x-ray emission MLD intensity given by

$$I(\theta) = (1 + \cos^2 \theta) \cdot F_{\pm 1,q} + (2 \sin^2 \theta) \cdot F_{0,q}. \qquad (3)$$

If the emission angle θ equals 90°, the emitted x-ray is equal to $F_{\pm 1q} + 2F_{0q}$. If θ equals zero, it is $2F_{\pm 1q}$. The MLD spectral shape is given by the difference between $\theta=0°$ and $\theta=90°$. It is equal to $F_{\pm 1,q} - 2F_{0,q}$.[3] Because of spatial limitations, the experiments have been carried out at angles of $\theta=70°$ and $\theta=30°$. This implies that the absolute MLD intensity is reduced by a factor of 0.63 with respect to measurements performed at 0° and 90°, while the MLD spectral shape remains the same.

A. Symmetries

The ground state is described as Yb^{3+} ions with $4f^{13}$ [$^2F_{7/2}$] symmetry. The intermediate state is $2p^5 4f^{13}$ plus a continuum electron that will be neglected in the following. The most important interaction in the intermediate state is the $2p$ spin-orbit coupling (ξ_{2p}). The binding energies for the $2p$ core states are, respectively, 8943 eV for $2p_{3/2}$ and 9978 eV for $2p_{1/2}$, with the energy separation of 1035 eV given by $\frac{3}{2}\xi_{2p}$. Because of the relatively small coupling of the $2p$ and $4f$ electrons, it can be assumed that the symmetry of the $4f$ electrons is not modified in the excitation process.[11] Only the $2p$ and $4f$ spin-orbit couplings are important and the symmetries of the intermediate state are best given in jj coupling. The symmetry is given by the multiplication of the $2p_{1/2}$ and $4f_{7/2}$ states, which implies that the intermediate states must have a J value of 3 or 4. The $4d^9 4f^{13}$ final state has a very large overlap between the $4d$ and $4f$ wave functions. As a result the energy states are spread over an energy range of some 20 eV. The $4d4f$ overlap is described with the two-electron $F_{2,4}$ and $G_{1,3,5}$ Slater parameters.[11] The (Coulomb) Slater parameters are $F_2 = 19.4$ and $F_4 = 12.4$ and the (exchange) Slater parameters are $G_1 = 22.7$, $G_3 = 14.4$, and $G_5 = 10.2$ eV. These values
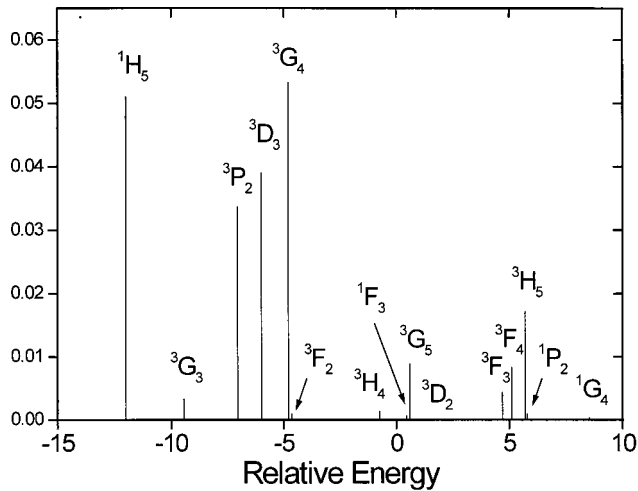
FIG. 2. The theoretical result for the $2p_{1/2}4f^{13} \rightarrow 4d^9 4f^{13}$ dipole transition. The energy scale is referenced to the average energy of the final state. The relative cross sections are given for the 15 term symbols acquiring finite intensity.

have been reduced to 80% of their Hartree-Fock values.[13] The atomic $4d$ and $4f$ spin-orbit couplings are, respectively, 3.58 and 0.40 eV. Because the spin-orbit interactions are smaller then the Slater parameters, the symmetry of the final states can be described best with $^{2S+1}L_J$ term symbols. The actual states are in general more than 90% pure in a particular $^{2S+1}L_J$ symmetry. Figure 2 gives the final-state term symbols and their intensity resulting from the calculation of the $|\langle 4d^9 4f^{13}|C_{q'}|2p_{1/2}4f^{13}\rangle|^2$ matrix elements. The average energy of the final state has been set to zero. The energy axis of the figures is given such that the state with the highest binding energy is at the left side of the figure (as it is closest to the $2p$ state). It can be checked that by multiplying the ^2D character ($4d^9$ electronic configuration) with the ^2F character ($4f^{13}$ electronic configuration), one finds singlet and triplet P, D, F, G, and H states. After inclusion of spin-orbit coupling, one obtains 20 $^{2S+1}L_J$ states. Since the $2p4f$ state has J values of 3 and 4, the dipole selection rule implies that the J value of the final state must be 2, 3, 4, or 5. One is then left with 15 term symbols that acquire intensity, whereas the other five term symbols (respectively $^3H_6$, $^1P_1$, $^3P_0$, $^3P_1$, and $^3D_1$) have zero intensity. Because the Hunds rule $^3H_6$ state has zero intensity, the $^1H_5$ state has the highest binding energy.

B. Comparison between theory and experiment

The theoretical stick spectrum has been convoluted with a Lorentzian broadening of 2.5 eV (half width at half maximum) and a Gaussian broadening of 1.5 eV (full width at half maximum). The Lorentzian broadening arises from both the lifetime broadening of the $2p$ hole (about 2.0 eV) and the lifetime broadening of the $4d$ hole (approximated to 0.5 eV). The Gaussian broadening simulates the experimental resolution. The MLD curve has been calculated by adding a magnetic field in the z direction and determining the difference between the $q = \pm 1$ and $q = 0$ cases of the $|\langle 4d^9 4f^{13}|C_{q'}|2p_{1/2}4f^{13}\rangle|^2$ matrix elements. The top panel of Fig. 3 shows the resulting theoretical spectrum (solid line)
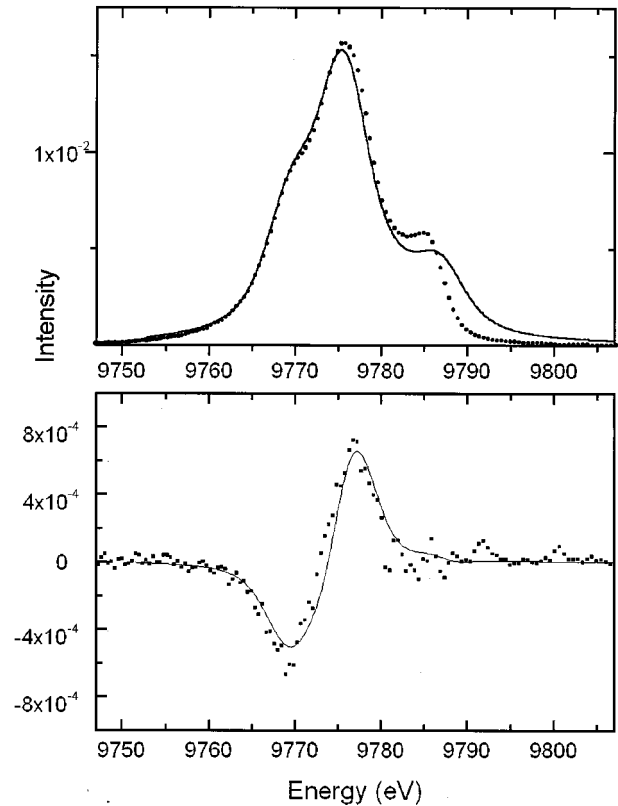

FIG. 3. Comparison of the $2p_{1/2}4d$ x-ray emission (top) and MLD (bottom) experimental spectral shape (dots) with the broadened theoretical spectrum (solid line). The theoretical MLD spectrum was divided by a factor 10 in order to match the intensity of the experimental spectrum (see text).

in comparison with the experimental curve (dots). The theoretical spectrum is averaged for all polarizations and the experimental spectrum is the (magic-angle) average of the spectra taken at 70° and 30°.

The shoulder at 9770 eV is related to the $^1H_5$ state (cf. Fig. 2) and the main peak around 9775 eV is related to the combination of the three triplet states $^3P_2$, $^3D_3$, and $^3G_4$. The satellite at 9785 eV arises from a superposition of all the low-intensity states in this region. Its energy position is slightly overestimated in the calculation. We believe this discrepancy to be due to uncertainties in the values of the Slater integrals, which have been determined with the rather crude method of the 80% reduced Hartree-Fock values. Another possibility involves intermediate state screening effects that were found important, for example, in the x-ray emission spectral shape of nickel compounds.[14] The bottom panel of Fig. 3 shows the theoretical (solid line) and experimental (dots) magnetic linear dichroism spectrum. As for the emission spectrum, the agreement is very good. The MLD spectrum shows essentially a negative peak at the $^1H_5$ state, a positive peak at the triplet states and an almost zero MLD between 9780 and 9785 eV.

The intensity of the theoretical x-ray emission spectrum has been multiplied by 0.08. This factor of 0.08 originates from two effects. The first factor is that the measurements are taken at 70° and 30°, while the theory applies for 0° and 90°. This reduces the effect by a factor of 0.63. The second

factor is the incomplete magnetization of the Yb sublattice at 90 K. According to the magnetization curves of Yb and Y iron garnet,[15] and assuming an equivalent iron magnetization in both samples, the magnetization of Yb is only approximately 0.12 of its maximal magnetization. Combining both factors, the theoretical curve should be multiplied with a factor of 0.08 to compare to experiment. Comparison between the theoretical and experimental MLD spectra shows good agreement for the spectral shape and reasonable agreement for the absolute intensity. The absolute intensity comparison suffers from the uncertainty in the detection angles and the detection angle spread, and in addition from the broadening applied to the theoretical spectrum. Taken together this creates an error margin estimated to be some 10–15%. Thus within this margin it is possible to determine the absolute magnetic Yb $4f$ moment. These uncertainty factors are not depending on temperature, implying that the relative uncertainty in temperature variations of the Yb $4f$ moment determination will be significantly smaller.

IV. DISCUSSION

A. Comparison between MLD and MCD

In the following, we discuss the difference between this MLD experiment and the MCD x-ray emission experiments, carried out for Gd metal in one of our previous papers.[11] In the MCD experiments, circularly polarized x rays impinging on a magnetized sample are used to excite $2p$ core electrons into empty states well above the edge. Subsequently an x-ray emission channel, corresponding to the radiative decay of a shallower core level electron into the $2p$ core level, is detected. In the present case of the Yb $2p_{1/2}4d$ x-ray emission, this would imply the use of circularly polarized x rays of 10 070 eV with the detection of the x-ray emission spectral shape at its magic angle.[11] In this context the magic angle detection is necessary in order to rule out any angular dependent effects. In these MCD experiments the dichroism is part of the excitation step, while in the emission MLD effects discussed above, the linear dichroism is part of the decay step. It is possible to make all kind of combinations of dichroism in excitation and dichroism in decay, but we leave this out of the present discussion. Emission MLD is equal to $F_{\pm 1,q} - 2F_{0,q}$ and MCD is equal to $F_{q',-1} - F_{q',+1}$, with q and q' ranging over all possible values (-1, $+1$, and 0).[11]

Figure 4 shows the calculated intensities of the 15 final states in the case of emission MLD (top panel), MCD (middle panel), and x-ray emission for the Yb $2p_{1/2}4d$ channel (cf. Fig. 2). It can be seen that the behavior of the individual term symbols differs. Concentrating only on the four major peaks between -12 and -5 eV, the $^1H_5$ state (cf. Fig. 2) has a negative contribution in both MCD and emission MLD. The $^3P_2$ state is negative in emission MLD, but is positive in MCD, the $^3D_3$ state is positive in both cases, and the $^3G_4$ is positive in emission MLD, whereas it is close to zero in MCD. In the case of MCD, this can be understood since the J value of the state is essentially determining the sign of the MCD, and high J-value term symbols have a negative MCD effect. Figure 5 shows the broadened Yb $2p_{1/2}4d$ x-ray emission spectrum and its MCD and emission MLD effects. Both dichroism spectra do follow the same
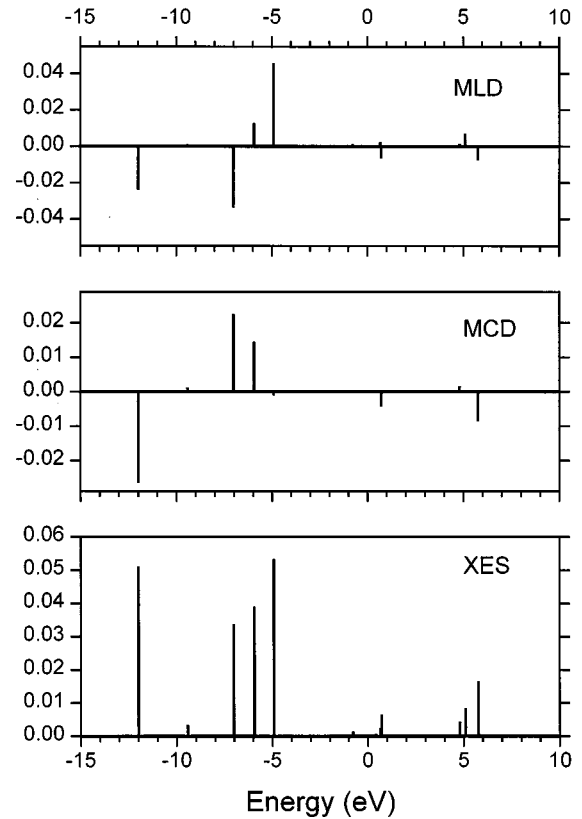

FIG. 4. The theoretical $2p_{1/2}4d$ x-ray emission lines (bottom), their MCD effects (middle), and emission MLD effects (top).

general trend of a negative peak at the $^1H_5$ state and a positive peak at the triplet states, but their detailed spectral shapes are rather different.

We note that both the MCD and the emission MLD integrated intensities are equal to zero. In the case of emission MLD this is evident, as the total x-ray emission integrated over an edge must be spherically symmetric, because only core levels are involved in the x-ray emission process itself. This implies a zero integrated intensity over the MLD effect in the $2p4d$ x-ray emission spectrum. In principle, one could envisage a finite emission MLD effect for the $2p_{1/2}$ edge, which would be compensated at the $2p_{3/2}$ edge, similar to the situation in the MCD of soft x-ray absorption. The $2p$ spin-orbit coupling, however, is so large that the $2p_{1/2}$ and $2p_{3/2}$ states can be assumed to be pure, implying zero integrated intensity for the emission MLD effect. The same is true for the MCD effect, as the electron is excited from a core state to a continuum state some 100 eV above the edge, where no significant MCD effect is expected in the absorption. While the integrated intensity of the MCD and emission MLD effects is zero, their amplitude is proportional to the $4f$ magnetization, because it is the $4d4f$-exchange interaction which gives rise to the appearance of the dichroism signal. It therefore shares this sensitivity with the $3d$ and $4d$ absorption MCD and absorption MLD spectra of the rare earths.

B. $2p4d$ emission MLD in comparison with $2p$ absorption MCD

The comparison between $2p4d$ emission MLD and $2p$ absorption MCD needs some extra discussion. $2p$ absorption
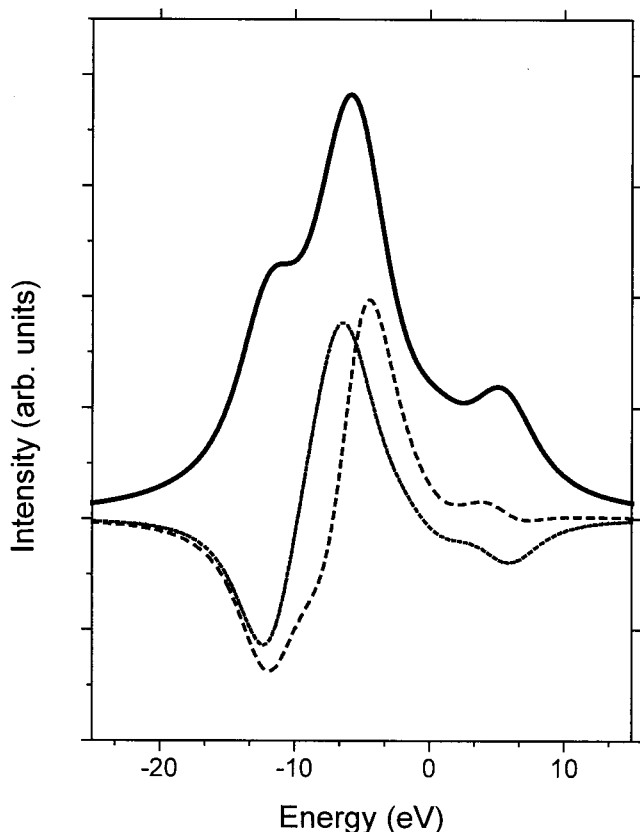
FIG. 5. The broadened $2p_{1/2}4d$ x-ray emission spectrum (solid line), its absorption MCD spectrum (dashed line) and emission MLD spectrum (dotted line). The two dichroic spectra have been multiplied by a factor 2 for clarity.

MCD is an often studied spectrum in magnetism studies of rare earths.[16] The modelling of $2p$ absorption MCD, including its associated magnetic sum rules, has been the topic of a range of theoretical studies.[17,18] Concerning the size of the $2p$ absorption MCD effect, a central role in these studies is played by the $4f5d$ exchange interaction. The $2p$ absorption spectrum is dominated by electric dipole transitions into the $5d$ band, while its corresponding MCD spectrum is largely influenced by the partly filled $4f$ states, which affect the $5d$ states via $4f5d$ exchange. An important question is if the size of the $2p$ absorption MCD follows the $4f$ moment or the $5d$ (or total) moment. From recent experimental studies, a contradictory result is found. A study on Gd-Fe-garnet $Gd_3Fe_5O_{12}$ clearly shows that the $2p$ absorption MCD scales with the $4f$ moment,[19] while a study on the same Gd L_2 edge for GdNiCo intermetallics shows that the $2p$ absorption MCD scales with the total moment.[20] The only explanation we could envisage combining both results is that the magnetic couplings are different in oxides then in intermetallics due to the different behavior of the $5d$ electrons. It would be very interesting to see more experimental evidence on this point.

The situation for $2p4d$ emission MLD is different. As discussed above, here the $4d4f$ exchange creates the magnetic effect. The $4d4f$ exchange is an atomic effect that is not affected by any modifications in the $5d$ valence band. Therefore the $2p4d$ emission MLD will scale with the $4f$

moment of the rare earth, independent of the system being an intermetallic or an oxide. This scaling with the $4f$ moments is thus the same as observed for oxides,[19] but different as observed for intermetallics.[20]

C. A spectroscopic tool

From this analysis, the size of the emission MLD effect appears as a property that is sensitive to the $4f$ magnetic moments of the rare earths. This technique is therefore complementary to absorption MLD or MCD spectroscopies at the rare earth $3d$ and $4d$ edges, which have to be performed in the soft x-ray regime. Note that for each rare-earth element a variety of possible x-ray emission channels are available, respectively the $2p_{1/2}4d$, $2p_{3/2}4d$, $2p_{1/2}3d$, and $2p_{3/2}3d$ channels. Each of these channels has a finite intensity for its emission MLD effect. The choice what channel to use can be made from the analysis of the theoretical spectral shapes and the appropriateness of the energies involved for the experimental setup. From the analysis of the spectral shape, one can conclude that for a measurement of the peak intensity itself one does not need a very good resolution. One could, for example, put a 5-eV window around both the positive peak and the negative peak and detect for these two windows the intensity at two angles. By doing so, one could vary the temperature, the pressure or the magnetic field, and follow the size of the magnetic moment. This technique can obviously be extended to $3d$ transition-metals systems where the $1s2p$ and $1s3p$ x-ray emission channels will have a MLD effect that is, in this case, sensitive to the $3d$ magnetic moment.

V. CONCLUDING REMARKS

We have shown that it is possible to measure a magnetic linear dichroism effect in the $2p_{1/2}4d$ x-ray emission spectrum of Yb. The spectral shape can be well reproduced using an atomic multiplet calculation of the $2p$ to $4d$ decay. The details of the spectral shapes are determined by the $4d4f$ exchange interaction. While the integrated intensity of the MLD effect is zero, the magnitude of the effect is a direct measure of the $4f$ magnetic moment of Yb. This technique can be generally applied to all rare earths and transition metals where four respectively two different emission channels can be utilized. Magnetic linear dichroism in x-ray emission promises to become a useful technique in the study of magnetic materials, since it circumvents the intrinsic complications of soft x-ray spectroscopies such as high vacuum environment and electron detection. Furthermore, the use of hard x rays implies that the technique is a bulk sensitive probe. Consequently, buried layers or interfaces are accessible for studies and measurements of systems under high pressure and temperature are feasible.

The experiment has been performed with an incident photon flux of 3×10^{12} photons/sec and a typical $2p4d$ x-ray emission spectrum as shown in Fig. 3 needs some 5 h counting time. This implies that the overall experiment detected at two angles and cross checked by flipping the magnetic field takes 20 h or some 10^{17} photons. Because the experiment makes use of an off-resonant excitation, one could signifi-

cantly increase the incident photon flux and thus decrease the data acquisition time by, i.e., using the full width of an undulator harmonic or the white spectrum of a bending magnet source. One might even think of using a laboratory source though the time needed to obtain 10^{17} photons will probably

be too long for practical studies. In conclusion, we state that although these experiments are not easy to perform because of the need of high photon flux and an efficient x-ray emission spectrometer, the potential applications are very promising.

[1] G. Schütz, W. Wagner, W. Wilhelm, P. Kienle, R. Zeller, R. Frahm, and G. Materlik, Phys. Rev. Lett. **58**, 737 (1987).

[2] G. van der Laan, B. T. Thole, G. A. Sawatzky, J. B. Goedkoop, J. C. Fuggle, J. M. Esteva, R. Karnatak, J. P. Remeika, and H. A. Dabkowska, Phys. Rev. B **34**, 6529 (1986).

[3] J. B. Goedkoop, B. T. Thole, G. van der Laan, G. A. Sawatzky, F. M. F. de Groot, and J. C. Fuggle, Phys. Rev. B **37**, 2086 (1988).

[4] B. T. Thole and G. van der Laan, Phys. Rev. Lett. **67**, 3306 (1991).

[5] Ch. Roth, H. B. Rose, F. U. Hillebrecht, and E. Kisker, Solid State Commun. **86**, 647 (1993).

[6] G. van der Laan, J. Magn. Magn. Mater. **148**, 53 (1995).

[7] J. Vogel and M. Sacchi, Surf. Sci. **365**, 831 (1996).

[8] Jan Vogel, Ph.D. thesis, University of Nijmegen, 1994.

[9] C. F. Hague, J.-M. Mariot, P. Strange, P. J. Durham, and B. L. Gyorffy, Phys. Rev. B **48**, 3560 (1993).

[10] M. Krisch, F. Sette, U. Bergmann, C. Masciovecchio, R. Verbeni, J. Goulon, W. Caliebe, and C. C. Kao, Phys. Rev. B **54**, 12 673 (1996).

[11] F. M. F. de Groot, M. Nakazawa, A. Kotani, M. H. Krisch, and F. Sette, Phys. Rev. B **56**, 7285 (1997).

[12] T. Åberg and B. Crasemann, in *X-ray Anomalous (Resonance) Scattering: Theory and Experiment*, edited by K. Fisher, G. Materlik, and C. Sparks (Elsevier, Amsterdam, 1994).

[13] F. M. F. de Groot, J. Electron Spectrosc. Relat. Phenom. **67**, 529 (1994).

[14] F. M. F. de Groot, A. Fontaine, C. C. Kao, and M. Krisch, J. Phys.: Condens. Matter **6**, 6875 (1994).

[15] C. Kittel, *Introduction to Solid State Physics*, 7th ed. (Wiley, New York, 1996).

[16] F. Baudelet, C. Giorgetti, S. Pizzini, C. Brouder, E. Dartyge, A. Fontaine, J. P. Kappler, and G. J. Krill, J. Electron Spectrosc. Relat. Phenom. **62**, 153 (1993).

[17] T. Jo and S. Imada, J. Phys. Soc. Jpn. **62**, 3721 (1993).

[18] M. van Veenendaal, J. B. Goedkoop, and B. T. Thole, Phys. Rev. Lett. **78**, 1162 (1997).

[19] J. B. Goedkoop, A. Rogalev, M. Rogaleva, C. Neumann, J. Goulon, M. van Veenendaal, and B. T. Thole, J. Phys. IV **7**, 415 (1997).

[20] J. P. Rueff, R. M. Galera, S. Pizzini, A. Fontaine, L. M. Garcia, C. Giorgetti, E. Dartyge, and F. Baudelet, Phys. Rev. B **55**, 3063 (1997).